# Determination of Iron−Ligand Bond Lengths in Ferric and Ferrous Horse Heart Cytochrome *c* Using Multiple-Scattering Analyses of XAFS Data

**Ming-Chu Cheng, Anne M. Rich, Robert S. Armstrong,* Paul J. Ellis, and Peter A. Lay***

School of Chemistry, University of Sydney, Sydney, NSW 2006, Australia

*Received April 9, 1999*

X-ray absorption fine structure (XAFS) data were obtained from frozen aqueous solutions (10 K) of horse heart ferri- and ferrocyt *c*. Models of the structure about the Fe center were refined to optimize the fit between the observed XAFS in the range $0 \leq k \leq 16.3$ Å$^{-1}$ and the XAFS calculated using both single-scattering (SS) and multiple-scattering (MS) calculations. The bond lengths obtained are more accurate and precise than those determined previously for cyt *c* from various species using X-ray crystallography. The Fe−N bond lengths are 1.98−1.99 Å for both oxidation states of cyt *c*. The Fe−S bond of ferricyt *c* (2.33 Å) is significantly longer than that of ferrocyt *c* (2.29 Å). The small changes in the bond lengths are consistent with the small reorganizational energy required for the fast electron-transfer reaction of cyt *c*.

## Introduction

Cytochrome *c* (cyt *c*) is a small heme protein (MW 12 384) that functions as a biological electron-transfer agent. It consists of a single polypeptide chain and a prosthetic heme group and provides a pathway for the transfer of electrons from cyt *c* reductase to cyt *c* oxidase in the mitochondrial respiratory chain (oxidative phosphorylation). The protein participates in oxidation−reduction reactions with the heme iron alternating between the oxidized (ferric, $Fe^{III}$) state and the reduced (ferrous, $Fe^{II}$) state. In the native protein, histidine 18 and methionine 80 of the protein chain are bound as axial ligands to produce a six-coordinate Fe center. Crystallographic studies of horse heart ferricyt *c* culminated in 1971 in a 2.8-Å-resolution structure determination that defined the general folding characteristics of this class of protein.[1] No further analyses appeared until 1981, when the three-dimensional structure of tuna ferrocyt *c* was refined at a resolution of 1.5 Å.[2] In 1990, the three-dimensional structure of horse heart ferricyt *c* was refined at 1.94-Å resolution.[3] Recently, the structures of horse heart ferri- and ferrocyt *c* have also been determined by high-resolution NMR spectroscopy.[4]

The macromolecular crystallographic and NMR results reported to date have not determined Fe−ligand bond lengths of the cyt *c* with sufficient accuracy and precision to identify small heme stereochemical differences that might accompany a change in oxidation state. X-ray absorption fine structure (XAFS) spectroscopy is capable of detecting such differences. XAFS spectroscopy has been used to obtain average metal−ligand bond lengths from proteins in solution with an accuracy of better than 0.02 Å.[5] In 1982, Korszun et al. obtained XAFS fluorescence spectra from several *c*-type cytochromes. One-shell analyses yielded average Fe−N bond lengths of 1.97−1.99 Å and Fe−S bond lengths of 2.29−2.32 Å, with estimated errors of about 0.02−0.03 Å.[6]

Because no crystal structures of sufficient resolution to permit the detection of small structural changes between ferri- and ferrocyt *c* are available, it was decided to examine the differences in the coordination site of the two oxidation states from a single species with MS XAFS analyses.[7] Such MS XAFS analyses with restrained and constrained bond angles and distances for heme proteins and porphyrins were described in detail in the early 1990s.[8−10] The current studies on cyt *c* were also of interest as a precursor for using XAFS to examine conformational changes in cyt *c* and to study their NO adducts along the lines reported for myoglobin (Mb).[11] The new Fe−ligand distances are compared with those obtained by X-ray crystallography, antecedent SS analyses, and SS analyses of our own XAFS data.

## Experimental Section

**Sample Preparation.** Horse heart cyt *c* (Sigma) was used without further purification. Native ferricyt *c* was dissolved in sodium phosphate buffer (0.1 M, pH 6.9), and its concentration was determined using the following molar absorptivities: $\epsilon_{410} = 106.1$ mM$^{-1}$ cm$^{-1}$, $\epsilon_{528} = 11.2$ mM$^{-1}$ cm$^{-1}$.[12]

Ferrocyt *c* was prepared by reducing the ferric form with a 6-fold molar excess of aqueous $Na_2S_2O_4$. This involved deoxygenating

(1) Dickerson, R. E.; Takano, T.; Eisenberg, D.; Kallai, O. B.; Samson, L.; Cooper, A.; Margoliash, E. *J. Biol. Chem.* **1971**, *246*, 1511−1535.
(2) Takano, T.; Dickerson, R. E. *J. Mol. Biol.* **1981**, *153*, 79−94.
(3) Bushnell, G. W.; Louie, G. V.; Brayer, G. D. *J. Mol. Biol.* **1990**, *214*, 585−595.
(4) (a) Qi, P. X.; Di Stefano, D. L.; Wand, A. J. *Biochemistry* **1994**, *33*, 6408−6417. (b) Qi, P. X.; Beckman, R. A.; Wand, A. J. *Biochemistry* **1996**, *35*, 12275−12286. (c) Banci, L.; Bertini, I.; Gray, H. B.; Luchinat, C.; Reddig, T.; Rosato, A.; Turano, P. *Biochemistry* **1997**, *36*, 9867−9877.
(5) Shulman, R. G.; Eisenberger, P.; Kincaid, B. M. *Annu. Rev. Biophys. Bioeng.* **1978**, *7*, 559−578.
(6) Korszun, Z. R.; Moffat, K.; Frank, K.; Cusanovich, M. A. *Biochemistry* **1982**, *21*, 2253−2258.
(7) Rich, A. M.; Armstrong, R. S.; Ellis, P. J.; Freeman, H. C.; Lay, P. A. *Inorg. Chem.* **1998**, *37*, 5743−5753.
(8) Hasnain, S. S.; Strange, R. W. In *Biophysics and Synchrotron Radiation*; Hasnain, S. S., Ed.; Ellis Horwood Ltd.: Chichester, U.K., 1990; Chapter 4.
(9) Binsted, N.; Strange, R. W.; Hasnain, S. S. *Biochemistry* **1992**, *31*, 12117−12125.
(10) Chance, M. R.; Miller, L. M.; Fischetti, R. F.; Scheuring, E.; Huang, W.-X.; Sclavi, B.; Sullivan, M. *Biochemistry* **1996**, *35*, 9014−9023.
(11) Rich, A. M.; Armstrong, R. S.; Ellis, P. J.; Lay, P. A. *J. Am. Chem. Soc.* **1998**, *120*, 10827−10836.
(12) Margoliash, E.; Frohwirt, N. *Biochemistry* **1959**, *71*, 570−572.

10.1021/ic990395r CCC: $18.00 
Published on Web 11/23/1999

solutions (Ar) of ferricyt *c* and $Na_2S_2O_4$ in buffer prior to mixing them under Ar. The concentration of native ferrocyt *c* was determined on the basis of: $\epsilon_{416} = 129.1\ mM^{-1}\ cm^{-1}$, $\epsilon_{550} = 27.7\ mM^{-1}\ cm^{-1}$.[12]

The final concentrations of the freshly prepared ferri- and ferrocyt *c* solutions, after the addition of glycerol (AR grade) to produce a 40% v/v glycerol/water mixture, were 7.1 and 4.3 mM, respectively. The solutions were syringed into 140-$\mu$L Lucite XAFS cells (23 × 2 × 3 mm) with 63.5-$\mu$m Mylar tape windows, frozen in a liquid $N_2$/*n*-hexane slush bath to form a homogeneous glass, and stored in liquid $N_2$ prior to inserting them into the liquid He cryostat for data collection. For ferrocyt *c*, the glycerol was deoxygenated (Ar) and all manipulations were performed under Ar.

**Data Collection.** Fe K-edge X-ray absorption spectra were recorded at the Stanford Synchrotron Radiation Laboratory (SSRL) on the unfocused beamline 7-3, using a Si(220) double-crystal monochromator detuned 50% at 8243 eV. Data were collected for ferri- (39 scans) and ferrocyt *c* (21 scans) as fluorescence spectra in the region 6790−8243 eV using a 13-element Ge array detector. To monitor photodecomposition of the samples during data collection, individual scans were energy-calibrated and compared using the programs XAS-Collect[13] and EXAFSPAK.[14] If a shift in the edge of >0.5 eV was observed, either the sample was translated to place the X-ray beam on a fresh spot or a new sample was used. A constant temperature of 10 K was maintained using an Oxford Instruments continuous-flow-liquid-helium CF 1208 cryostat. All spectra were energy-calibrated using an Fe foil standard, with the first inflection point of the foil spectrum assigned as 7111.2 eV.[15]

The scans obtained for each ferri- and ferrocyt *c* were averaged using weights based on the signal-to-noise ratios, and monochromator glitches were removed. A background correction was applied by fitting a third-order polynomial to the postedge absorbance and subtracting it from the data.[16] A three-region spline was fitted to the XAFS region and was then subtracted. The data were normalized to an edge jump of 1.0 and were compensated for decreasing absorbance past the edge.

**XAFS Model.** In heme proteins, atoms up to 5 Å from the Fe center may make significant MS contributions.[17] This distance generally captures all of the atoms of the porphyrin core and any exogenous ligands. For the MS analyses, the model for the Fe center in cyt *c* comprised an unsubstituted Fe porphyrin, the imidazole ring of a histidine side chain, and the four atoms of the methionine side chain. The porphyrin model that was used[7,16] is based on average bond distances and angles from six-coordinate [Fe(tetraphenylporphyrinato-(2−))] structures.[18−21] The porphyrin was constrained to be planar and maximally symmetric. Although this model has fewer adjustable parameters than one based on the unsymmetrical natural prosthetic group, protoporphyrin IX, the bond lengths obtained from the two models have been shown to be the same within experimental error for other heme proteins.[7,16] The bond lengths and angles for the imidazole (ImH) ligand were taken from ImH in $[Mn(ImH)_6]Cl_2 \cdot 4H_2O$.[22] The bond lengths and angles for the side chain of the methionine group were obtained from a statistical analysis of 541 entries of similar X-ray crystal structures from the Cambridge Structural Database System.[23] The geometry of the starting model is shown in Figure 1.

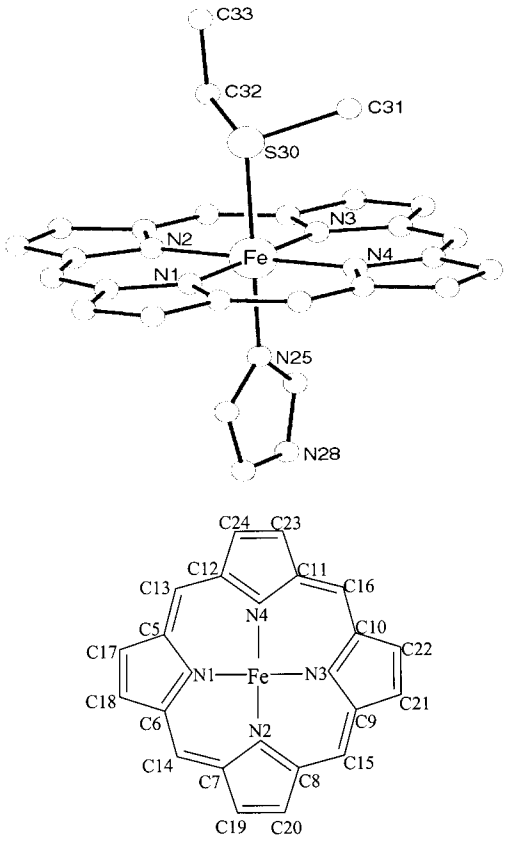


**Figure 1.** Starting model for cyt *c*.

**Data Analysis.** The model-fitting calculations were performed by means of the program XFIT,[24] which incorporates ab initio calculation of the XAFS using the SS (version 4.06)[25] and MS (version 6.01) of FEFF.[26] XFIT uses nonlinear least-squares fitting to vary model parameters to optimize the agreement between the observed and calculated XAFS.

In XFIT, restraints, which specify targets for relationships between model parameters, are used to incorporate prior information into an analysis.[24] The weight of each restraint expression is given by $1/\sigma_{res}^2$, where the parameter $\sigma_{res}$ is given in Table S1 (Supporting Information) and is analogous to an estimated standard deviation. Thus, the larger the value of $\sigma_{res}$, the greater the freedom of movement of the bond length or angle from the specified value. The value of $\sigma_{res}$ is chosen to ensure that bond lengths and angles stay within the normal bounds found within ligands and hence prevents a chemically unreasonable fit to the data. The weight of the XAFS data relative to the restraints in the fitting procedure is given by a separate weighting factor *w*. The higher the value of *w*, the lower the importance placed on maintaining the restraints during the fitting procedure.[24] Throughout the refinements, *w* was fixed at 8, giving differences between the refined and ideal values of the restraints close to the specified $\sigma_{res}$ values.

The bond lengths and bond angles within the porphyrin ligand were tightly restrained to the geometry of the model ($\sigma_{res} = 0.01$ Å and 1° for bond lengths and bond angles, respectively). Weaker restraints were placed on the bond lengths and angles between the pyrrole rings to allow them to move closer to, or further away from, the Fe atom ($\sigma_{res} = 0.02$ Å and 2° for bond lengths and bond angles, respectively). For all atoms except those in the imidazole ligand, the Debye−Waller

(13) George, M. J. *XAS-Collect: A Program for X-ray Absorption Spectroscopy Data Collection*, version 1.2; SSRL: Stanford, CA, 1995.
(14) George, G. N.; Pickering, I. J. *EXAFSPAK: A Suite of Computer Programs for Analysis of X-ray Absorption Spectra*; SSRL: Stanford, CA, 1995.
(15) Zhang, Y.; Pavlosky, M. A.; Brown, C. A.; Westre, T. E.; Hodgson, K. O.; Solomon, E. I. *J. Am. Chem. Soc.* **1992**, *114*, 9189−9191.
(16) Rich, A. M. Determination of Fe-Ligand Bond Lengths and Angles in Hemeproteins Using X-ray Absorption Spectroscopy. Ph.D. Thesis, University of Sydney, 1997.
(17) Pin, S.; Alpert, B.; Congiu-Castellano, A.; Longa, S. D.; Bianconi, A. *Methods Enzymol.* **1994**, *232*, 266−292.
(18) Mashiko, T.; Reed, C. A.; Haller, K. J.; Kastner, M. E.; Scheidt, W. R. *J. Am. Chem. Soc.* **1981**, *103*, 5758−5767.
(19) Scheidt, W. R.; Lee, Y. J. *Struct. Bonding* (*Berlin*) **1987**, *64*, 1−70.
(20) Mashiko, T.; Reed, C. A.; Haller, K. J.; Scheidt, W. R. *Inorg. Chem.* **1984**, *23*, 3192−3196.
(21) Radonovich, L. J.; Bloom, A.; Hoard, J. L. *J. Am. Chem. Soc.* **1972**, *94*, 2073−2078.
(22) Garrett, T. P. J.; Guss, J. M.; Freeman, H. C. *Acta Crystallogr., Sect. C* **1983**, *C39*, 1027−1031.
(23) *The Cambridge Structural Database System*; Cambridge Crystallographic Data Center: Cambridge, U.K., 1996.
(24) Ellis, P. J.; Freeman, H. C. *J. Synchrotron Radiat.* **1995**, *2*, 190−195.
(25) Mustre de Leon, J.; Rehr, J. J.; Zabinsky, S. I.; Albers, R. C. *Phys. Rev. B* **1991**, *44*, 4146−4156.
(26) Rehr, J. J.; Albers, R. C.; Zabinsky, S. I. *Phys. Rev. Lett.* **1992**, *69*, 3397−3400.

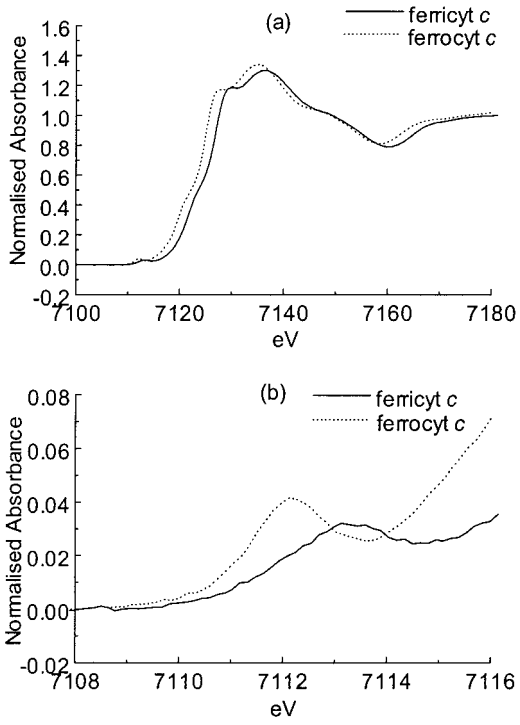


**Figure 2.** (a) Edge and (b) enlarged preedge spectra of cyt *c*.

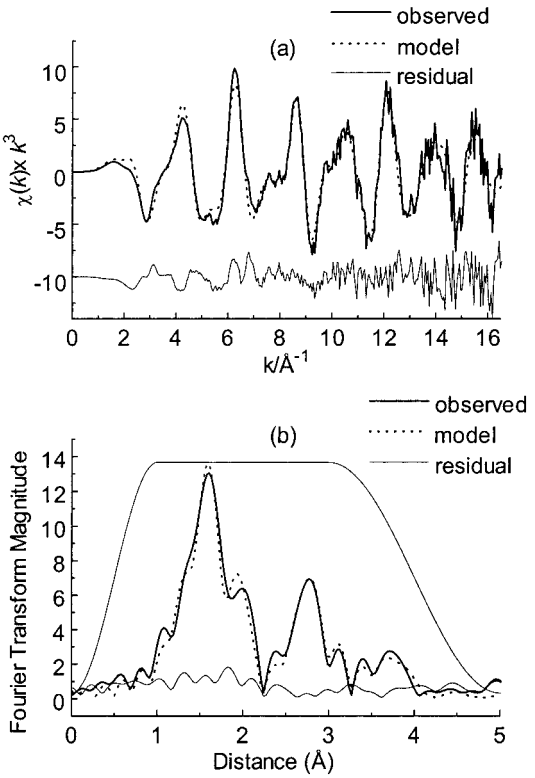


**Figure 3.** (a) XAFS and (b) Fourier transform amplitude of XAFS for ferricyt *c*.

factors, $\sigma^2$, were restrained to increase with each bond away from the Fe atom ($\sigma^2 = 0.001$ Å$^2$) to reflect the expected increase in static and dynamic disorder as the distance of the scatterer from the absorber increases.[27] For the imidazole ligand, the Debye−Waller factors were restrained to increase in the order $\sigma^2$(N25) < $\sigma^2$(N28, C29) < $\sigma^2$(C26, C27). This order results from the greater effect of the in-plane rocking vibrational modes on the second-shell Fe−C26 and Fe−C27 distances than on the third-shell Fe−N28 and Fe−C29 distances and the low amplitude of the internal ring vibrations.[7]

Unless stated otherwise, constraints were applied to keep the porphyrin group in the *x*,*y* plane and the imidazole in the *y*,*z* plane to ensure that the fit was well overdetermined. Such constraints are justified because it was shown previously[7] that the XAFS is insensitive to small movements of the Fe out of the heme plane or rotations and tilts of the imidazole ring. The S atom of the methionine group was constrained to be perpendicular to the porphyrin plane, but the other atoms were free to move within the restraints. A table of restraints and constraints is given in the Supporting Information (Table S1).

**Error Estimates from Noise in the Data.** Monte Carlo analyses were conducted to estimate the rms deviations in final parameters arising from the noise in the data.[27−29] For all refinements reported in this paper, two consecutive sets of 16 × 16 Monte Carlo cycles were executed using the procedures described previously[27−29] in which the effect on the bond lengths and angles obtained from different fits to the variation in the XAFS from the noise in the data were examined. The resulting rms errors were combined with typical systematic errors to obtain the final error estimates.[7]

## Results

**The Edge and Preedge Region.** Figure 2a shows the Fe K-edge XAS spectra of ferri- and ferrocyt *c*. The preedge region is enlarged and is shown in Figure 2b. There is an ∼1 eV shift to lower energy of the edge transition from ferricyt *c* to ferrocyt *c*. The symmetry-forbidden 1s → 3d transitions (∼7112 eV) occur at slightly higher energy for the ferricyt *c* compared to ferrocyt *c*. The intensities are similar for these two oxidation states but are somewhat higher for the ferrous form. Data from 39 scans from three samples of ferricyt *c* were obtained. From the first to last scan on each of two spots for each sample, shifts in the edge position of up to 0.5 eV were observed, consistent with significant photoreduction.

**Analysis of Photoreduction.** To investigate the effect of photoreduction on the analysis of the ferricyt *c*, XAFS analyses were performed on the averaged data for 16 scans (edge shift less than 0.2 eV), those for 23 scans (edge shift less than 0.3 eV), and those for all 39 scans (edge shifts up to 0.5 eV). While the lowest *R* value was obtained with the average of all 39 scans, the threshold energy for excitation of the core electron, $E_0$, decreased by 0.6 eV compared to that obtained when data from the 16 scans with lowest edge shift were used (Table 1). The final analysis used the data from these 16 scans only, being most reliable for ferricyt c. The data from all 21 scans for ferrocyt *c* were used since there was no edge shift within experimental error (≤0.08 eV).

**SS and MS Analyses.** The XAFS data for ferri- and ferrocyt *c* were refined using both SS and MS calculations. The SS analyses used only the first-shell atoms, consisting of the pyrrole N ($N_p$), the imidazole N ($N_\epsilon$), and the methionine S atoms. All the model atoms have significant MS contributions and were used in the MS analyses. The results of the SS and MS analyses and the literature values from the prior SS analyses of ferri- and ferrocyt *c* are listed in Table 1. For the MS analyses, the observed and calculated XAFS, the corresponding Fourier transforms, the residuals, and the window functions used in the Fourier filter for ferri- and ferrocyt *c* are shown in Figures 3 and 4, respectively. The refined atomic positional coordinates for both forms of cyt *c* are contained in the Supporting Information (Tables S2 and S3). The bond lengths and bond

(27) Ellis, P. J. Structural Studies of Metalloproteins Using X-ray Absorption Spectroscopy and X-ray Diffraction. Ph.D. Thesis, University of Sydney, 1995.
(28) Hammersley, J. M.; Handscomb, D. C. *Monographs on Applied Probability and Statistics, Monte Carlo Methods*; Chapman & Hall: London, 1965.
(29) Spiegel, M. R. *Schaum's Outline of Theory and Problems of Probability and Statistics*; McGraw-Hill: London, 1975.

**Table 1.** Fe-Site Dimensions in Ferric and Ferrous Cytochrome *c* As Determined by MS and SS XAFS Analyses

| | | Fe−ligand distances (Å) | | | Debye−Waller Factors $\sigma^2$ (Å$^2$) | | | other refinement parameters | | |
|---|---|---|---|---|---|---|---|---|---|---|
| protein | XAFS analysis | Fe−$N_p$ | Fe−$N_\epsilon$ | Fe−S | $N_p$ | $N_\epsilon$ | S | $E_0$ (eV) | $S_0^2$ | $R$ (%) |
| ferricyt *c* | previous SS[a] | 1.47(3) | | | | | | | | |
| | previous SS[b] | 1.98(1) | | 2.31(2) | | | | | | |
| | SS | 1.98(2) | 1.98(2) | 2.33(2) | 0.001 | 0.001 | 0.001 | 7122.7 | 0.79 | 22.5 |
| | MS[c] | 1.98(2) | 1.98(3) | 2.33(2) | 0.002 | 0.002 | 0.002 | 7126.5(5) | 0.95(2) | 16.3 |
| | MS[d,e] | 1.98(2) | 2.01(3) | 2.33(2) | 0.002 | 0.001 | 0.002 | 7126.2(5) | 0.97(2) | 15.8 |
| | MS[e,f] | 1.98(2) | 2.01(3) | 2.33(2) | 0.002 | 0.001 | 0.002 | 7125.9(5) | 0.96(2) | 14.4 |
| ferrocyt *c* | previous SS[a] | 1.47(3) | | | | | | | | |
| | previous SS[b] | 1.99(1) | | 2.31(3) | | | | | | |
| | SS | 1.99(2) | 1.99(3) | 2.28(2) | 0.001 | 0.001 | 0.003 | 7121.9 | 0.81 | 18.4 |
| | MS | 1.99(2) | 2.00(2) | 2.29(2) | 0.001 | 0.002 | 0.003 | 7125.3(2) | 0.96(2) | 12.5 |

[a] SS analyses of horse heart cyt *c* in 1979.[34] The value shown is without a phase shift correction. [b] SS analyses of tuna heart cyt *c* in 1982.[6] The quoted errors are probably much lower than the actual errors. [c] Data from 16 scans that were least affected by photoreduction (average shift from first scan ≤0.19 eV). [d] Data from 23 scans (average shift in edge from first scan ≤0.29 eV). [e] The Debye−Waller factor of atom C33 is unreasonable (>0.03 Å$^2$). [f] Data from all 39 scans (average shift in edge from first scan ≤0.50 eV).

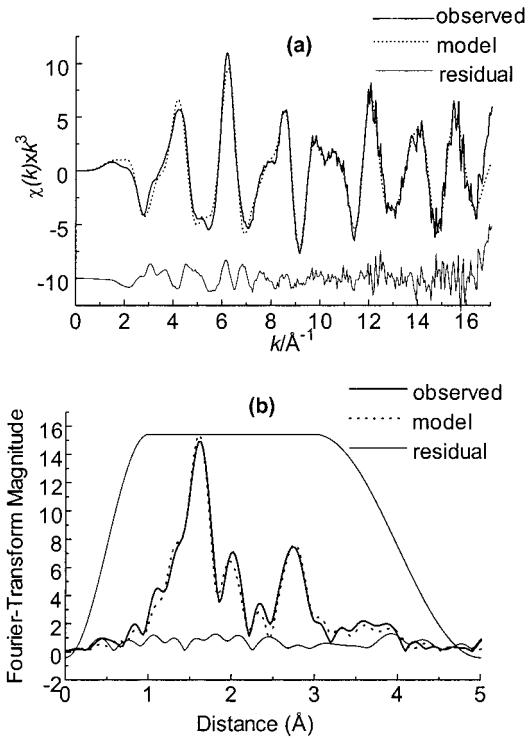


**Figure 4.** (a) XAFS and (b) Fourier transform amplitude of XAFS for ferrocyt *c*.

angles obtained from the MS analyses are compared with the X-ray crystal structures from the Brookhaven Protein Data Bank in Table 2.[30] Summaries of X-ray crystallographic data for ferri- and ferrocyt *c* from various species are presented in Tables 2 and S4, (Supporting Information), together with a determination of the precision of the atomic coordinates.[31]

The Fe−N distances obtained from SS calculations are in good agreement with those reported previously.[6] While the XRD and XAFS structures are not significantly different, the Fe−$N_p$ bond length (1.99 Å) of the ferrous form is shorter than that obtained from the crystal structure (2.04 Å), and the Fe−$N_\epsilon$ distance (1.98 Å) of ferricyt *c* is also shorter than that obtained from the X-ray crystal structure analysis (2.04 Å).[3] Previous SS analyses[6] indicated that the Fe−S bond length was about 2.31 Å for both oxidation states of cyt *c*. In this work, the Fe−S distance in the ferric form (2.33 Å) is longer than that in the ferrous form (2.28 Å).

The models obtained from the MS analyses gave good fits to the observed XAFS, with *R* values of 16.3% and 12.5% for ferri- and ferrocyt *c*, respectively, and the Debye−Waller factors are all low. The Fe−ligand bond length values are very close to those obtained from SS analyses and are in good agreement with the crystal structures, but the Fe−$N_\epsilon$ bond length (1.98 Å) for the ferric form is a little shorter than those in the crystal structures. The bond lengths and angles for the Fe−methionine moiety obtained from MS analyses are in excellent agreement with the crystal structures.

**Effect on the Fe−Ligand Distances of the Methionine Geometry Restraints.** Test refinements were performed to determine the effect of varying the geometry restraints applied to the methionine group. The refined Fe−ligand distances were insensitive to these restraints. Removal of S−C and C−S−C bond length and bond angle restraints had no effect on the Fe−ligand bond lengths (Supporting Information, Table S5). When the bond length and bond angle restraints on the methionine were removed, some of the C−S bond lengths were unreasonable; however, if only the bond angle restraints were released, the fit remained reasonable and Fe−S−C and C−S−C angles did not vary much between the two oxidation states.

**Effect on the Fe−Ligand Distances of Tilting the Imidazole Group.** The imidazole ring was tilted by up to 30° perpendicular to or within its plane, and the models were refined to convergence (Supporting Information, Table S6). These changes have no effect on the Fe−$N_p$ and Fe−S bond lengths, but the in-plane tilt has a significant effect on the Fe−$N_\epsilon$ distance (maximum change of 0.05 Å).

**Error Estimates.** The statistical errors from the Monte Carlo calculations[24,27] for ferric cyt *c* were 0.0035 Å for Fe−$N_p$, 0.013 Å for Fe−$N_\epsilon$, and 0.0025 Å for Fe−S. For ferrous cyt *c*, the errors were 0.0014 Å for Fe−$N_p$, 0.0033 Å for Fe−$N_\epsilon$, and 0.0016 Å for Fe−S. These statistical errors were combined with a conservative systematic error (±0.02 Å)[32] to obtain the estimated errors contained in the Table 1.

**Degree of Determinancy.** The number of parameters being refined, *p*, compared to the number of independent points, $N_i$, can be calculated to give the degree of determinancy, $N_i/p$. If this ratio is less than 1, the fit is underdetermined and a unique fit is not possible, whereas a ratio above 1 gives an overdetermined problem, which can be used to give a reliable fit. To

(30) Bernstein, F. C.; Koetzle, T. F.; Williams, G. J. B.; Meyer, E. F.; Brice, M. D.; Rodgers, J. R.; Kennard, O.; Shimanouchi, T.; Tasumi, M. *J. Mol. Biol.* **1977**, *112*, 535−542.

(31) Cruickshank, D. W. *Macromolecular Refinement*; SERC Daresbury Laboratory: Warrington, U.K., 1996; pp 11−22.

(32) Gurman, S. J. *J. Synchrotron Radiat.* **1995**, *2*, 56−63.

**Table 2.** Structural Data from MS XAFS Fits and X-ray Crystal Structures from the PDB for Ferri- and Ferrocyt *c*

| species | PDB entry[a] | Fe−$N_p$ (Å) | Fe−$N_\epsilon$ (Å) | Fe−S (Å) | S−C31 (Å) | S−C32 (Å) | C32−C33 (Å) | Fe−S−C31 (deg) | Fe−S−C32 (deg) | C31−S−C32 (deg) | S30−C32−C33 (deg) | *R* (%) | $\sigma$(x)[b] |
|---|---|---|---|---|---|---|---|---|---|---|---|---|---|
| | | | | | | Protein Ferricyt *c* | | | | | | | |
| horse heart | this work | 1.98 | 1.98 | 2.33 | 1.81 | 1.81 | 1.50 | 108 | 108 | 101 | 110 | 16.3 | |
| | 1HRC | 1.99 | 2.04 | 2.32 | 1.81 | 1.79 | 1.57 | 115 | 109 | 102 | 116 | 17.9 | 0.19 |
| | 1CRC (A)[c] | 1.98 | 1.96 | 2.02 | 1.81 | 1.83 | 1.49 | 106 | 125 | 95 | 110 | 17.7 | 0.57 |
| | 1CRC (B)[c] | 2.01 | 2.17 | 2.66 | 1.78 | 1.85 | 1.50 | 106 | 150 | 95 | 115 | 17.7 | 0.57 |
| rice embryos | 1CCR | 2.00 | 2.04 | 2.35 | 1.80 | 1.83 | 1.53 | 110 | 108 | 111 | 110 | 19.0 | 0.18 |
| tuna heart | 3CYT (O)[c] | 2.07 | 1.96 | 2.28 | 1.81 | 1.79 | 1.51 | 112 | 117 | 102 | 113 | 20.8 | 0.42 |
| | 3CYT (I)[c] | 2.03 | 2.04 | 2.26 | 1.77 | 1.79 | 1.49 | 114 | 120 | 105 | 110 | 20.8 | 0.42 |
| | | | | | | Protein: Ferrocyt *c* | | | | | | | |
| horse heart | this work | 1.99 | 2.00 | 2.29 | 1.82 | 1.81 | 1.50 | 109 | 109 | 101 | 110 | 12.5 | |
| bonito | 1CYC | 1.80 | 2.60 | 2.49 | 1.44 | | | 150 | | | | | |
| tuna heart | 5CYT | 2.04 | 1.98 | 2.31 | 1.80 | 1.81 | 1.54 | 115 | 116 | 105 | 115 | 17.3 | 0.085 |

[a] PDB = Brookhaven Protein Data Bank.[30] [b] Uncertainty $\sigma(x)$ in the position of an atom; $\sigma(x) = 1.0(N/P)^{1/2}C^{-1/3}d_{min}R$, where $P$ = no. of degrees of freedom = (no. of independent reflections − no. of variables); see Table S4. [c] There are two asymmetric molecules in the unit cell.

ensure that the problem is overdetermined for heme proteins,[9] constraints and restraints are required where the value of $N_i$ is given by

$$N_i = 2(\Delta r)(\Delta k)/\pi + \sum[D(N-2)+1] \qquad (1)$$

where $D$ is the number of dimensions in which the refinement takes place (2 for the planar porphyrin and imidazole units and 3 for the methionine group) and $N$ is the number of atoms in the unit. The model used in these calculations, together with the large $k$ range (16.3 Å$^{-1}$) of data used in the fit, results in a well-overdetermined MS XAFS fit ($N_i/p = 1.7$). This fit is much better overdetermined than those reported in the literature for heme proteins in the early 1990s,[8−10] largely due to improvements in the sensitivity of detection of XAFS, which enables data to be collected and analyzed over a larger $k$ range.

## Discussion

**XANES.** Although the edge features of both oxidation states of cyt *c* are similar, there are some characteristics of the preedge region that distinguish them. There is a weak preedge feature with a shoulder at lower energy for the ferricyt c that is a consequence of the low-spin ferric complex having a large number of one-electron allowed final states ($^1A_{1g}$, $^1T_{1g}$, $^3T_{1g}$, $^1T_{2g}$, and $^3T_{2g}$).[33] Experimentally, the $^1A_{1g}$ final state is at lower energy (~7110 eV) and is observed as a shoulder to the higher intensity peak containing contributions from the $^1T_{1g}$, $^3T_{1g}$, $^1T_{2g}$, and $^3T_{2g}$ final states. For the ferrocyt *c*, a feature on the rising edge of the spectrum at ~7115 eV is observed. This arises from the configurational mixing between the one-electron allowed $^2E_g$ state and higher energy two-electron $^2E_g$ excited state.[33−35] The difference in the energy of the edge is ~1 eV and, together with the preedge results and the UV/vis spectra, shows that the protein was fully reduced (>90%). This is important in establishing that the small differences observed in the bond length data were not due to incomplete reduction.

**XAFS.** The resulting values of *R* (the difference between the observed and calculated XAFS) of the MS analyses for ferricyt *c* (16.3%) and ferrocyt *c* (12.5%) are low, reflecting the high quality of the XAFS data and the fit to the data. With the exception of the Fe−$N_\epsilon$ bond length for ferricyt *c*, the bond distances determined are within experimental error of those found using X-ray crystallography. The most important aspect of the MS analysis is the small difference in the bond lengths and Fe−methionine angles between the two oxidation states. The resultant small inner-sphere reorganizational energy is a major reason for this metalloprotein undergoing fast electron transfer, as required for its physiological role.

While the major discrepancy between the XAFS and X-ray bond lengths is the value for the Fe−$N_\epsilon$ bond length in the ferric form, this may be a reflection of the quality of the X-ray structure. The diffraction precision indicator (DPI)[31] has been proposed by Cruickshank to estimate $\sigma_w(x)$, the uncertainty in the position of an average atom for the XRD data. Although the average uncertainty in the bond lengths are greater than the average uncertainty in the positional parameters, the Fe−L bond lengths are better defined than the average bond lengths; hence, the DPI has been used as an indication of the precision in these bond lengths.[7] While such an estimate is necessarily empirical, it is reasonable, given the large variations in the bond lengths determined in different structural determinations for a given protein, as has been analyzed in some depth for met- and deoxy-Mb.[7] For the XAFS-derived Fe−ligand bond lengths listed in Table 1, the probable errors were calculated from both random and systematic errors, with the latter dominating. Using a conservative consensus value 0.02 Å for the systematic error component,[32] overall probable errors in the range 0.02−0.03 Å were obtained for the Fe−ligand distances derived from the MS XAFS analyses. The general conclusion from Table 2 is that the best of the crystal structures have Fe−ligand bond length esd's of >0.1 Å. The esd's are in fact sufficiently large that, despite the range of values for each bond length, none of the bond lengths differs significantly from the values determined by XAFS analyses, nor are they precise enough to obtain reliable information as to the extent of bond length changes during electron transfer. Another problem with ascertaining bond length changes in XRD data is that, in the structures of horse heart and tuna heart ferricyt *c*, each has two asymmetric molecules in a unit with quite distinct Fe−$N_\epsilon$ bond lengths, i.e. 1.96 and 2.17 Å for horse heart ferricyt *c* and 1.96 and 2.04 Å for tuna heart ferricyt *c* (Table 2). This may be an artifact of the XRD results, as the XANES results at 10 K clearly show that there would be extensive photodamage at the Fe center for the ferricyt *c* during XRD data collection, which was performed at much higher temperatures than the XAS data collection. The low Debye−Waller factors and the excellent fit to the XAFS data show that there are not significant amounts of a second coordination geometry in the XAFS samples. SS analyses of

(33) Westre, T. E.; Kennepohl, P.; DeWitt, J. G.; Hedman, B.; Hodgson, K. O.; Solomon, E. I. *J. Am. Chem. Soc.* **1997**, *119*, 6297−6314.
(34) Labhardt, A.; Yuen, C. *Nature* **1979**, *11*, 150−151.
(35) Liu, H. J.; Sono, M.; Kadkhodayan, S.; Hager, L. P.; Hedman, B.; Hodgson, K. O.; Dawson, J. H. *J. Biol. Chem.* **1995**, *270*, 10544−10550.

XAFS data ($0 \leq k \leq 11$ Å$^{-1}$) on a range of cyt *c* proteins[6] showed a similar small change in bond lengths, as observed here using higher quality data and MS analyses. The small differences between the Fe−$N_p$ and the Fe−$N_\epsilon$ bond lengths mean that even MS analyses of the XAFS data cannot reliably distinguish between them. The small decrease in the Fe−S bond length in going from Fe(III) to Fe(II) is consistent with important $\pi$-back-bonding contributions in ferrocyt *c*, since such a bond would normally be expected to be shorter in the higher oxidation state. The importance of such $\pi$-back-bonding effects is consistent with the observation that the affinity of *N*-acetylmethionine for microperoxidase-8 increases with reduction of the heme.[36]

The tilt within the Fe−Im plane is close to zero for the average of three high-resolution cyt *c* structures (Table 2). This is in agreement with the XAFS results where tilts of $\geq 10°$ cause unrealistic Debye−Waller factors (Table S6).

**Conclusions.** Precise and accurate Fe−ligand bond lengths (particularly for Fe−$N_p$) can be obtained from MS analyses of heme protein XAFS data. The bond lengths obtained are more accurate than those determined from X-ray crystallographic data and show small differences in the bond lengths, consistent with near-zero reorganizational energy terms required for the fast electron-transfer properties of ferricyt *c* and ferrocyt *c*.

**Acknowledgment.** This work was supported by an Australian Research Council Grant (R.S.A. and P.A.L.) and by the Major Facilities Program funded by the Department of Industry, Science and Resources and managed by the Australian Nuclear Science and Technology Organisation. Additional funding was received through an Australian Postgraduate Research Award to A.M.R. We are grateful for the invaluable assistance provided by Professor Keith Hodgson and Dr. Britt Hedman at SSRL. Work was done partially at SSRL, which is operated by the Department of Energy, Office of Basic Energy Sciences. The SSRL Biotechnology Program is supported by the National Institutes of Health, National Center for Research Resources, Biomedical Technology Program, and by the Department of Energy, Office of Biological and Environmental Research.

**Supporting Information Available:** Tables of constraints and restraints for the parameters of cytochrome *c*, final refined atomic positional coordinates and X-ray crystallographic data for ferric and ferrous cyt *c*, and parameters used in the calculations of the DPI. This material is available free of charge via the Internet at htpp://pubs.acs.org.

IC990395R

(36) Texcan, F. A.; Winkler, J. R.; Gray, H. B. *J. Am. Chem. Soc.* **1998**, *120*, 13383−13388.